Isothermal and Nonisothermal Crystallization Kinetics of Isotactic Polypropylene Nucleated with Substituted Aromatic Heterocyclic Phosphate Salts

Yue-fei Zhang, Zhong Xin

UNILAB Research Center of Chemical Reaction Engineering, East China University of Science and Technology, Shanghai, 200237

Received 14 September 2005; accepted 17 November 2005
DOI 10.1002/app.23883
Published online in Wiley InterScience (www.interscience.wiley.com).

ABSTRACT: The crystallization kinetics of isotactic polypropylene (iPP) and nucleated iPP with substituted aromatic heterocyclic phosphate salts were investigated by means of a differential scanning calorimeter under isothermal and nonisothermal conditions. During isothermal crystallization, Avrami equation was used to describe the crystallization kinetics. Moreover, kinetics parameters such as the Avrami exponent n, crystallization rate constant Z_t, and crystallization half-time $t_{1/2}$ were compared. The results showed that a remarkable decrease in $t_{1/2}$ as well as a significant increase in overall crystallization rate was observed in the presence of monovalent salts of substituted aromatic heterocyclic phosphate, while bivalent and trivalent salts have little effect on crystallization rate of iPP. The addition of monovalent metal salts could decrease the interfacial free energy per unit area perpendicular to PP chains σ_e value of iPP so that the nucleation rate of iPP was increased. During nonisothermal crystallization, Caze method was used to analyze the crystallization kinetics. It also showed that monovalent metal salts had better nucleation effects than bivalent and trivalent metal salts. From the obtained Avrami exponents of iPP and nucleated iPP it could be concluded that the addition of different nucleating agents changed the crystal growth pattern of iPP. © 2006 Wiley Periodicals, Inc. J Appl Polym Sci 101: 3307–3316, 2006

Key words: crystallization kinetics; nucleating agent; isotactic polypropylene; substituted aromatic heterocyclic phosphate salts

INTRODUCTION

Sodium 2,2-methylene-bis (4,6-di-*tert*-butylphenyl) phosphate (commercial product name: ADK STAB NA-11) as a nucleating agent has been widely used in the modification of isotactic polypropylene (iPP) because they can improve the crystallization behaviors and mechanical properties of iPP remarkably.[1–6] In recent years, trivalent aluminum salts of 2,2-methylene-bis (4,6-di-*tert*-butylphenyl) phosphate used as a component of a novel nucleating agent (commercial product name: ADK STAB NA-21) has also been used for improving the transparency of iPP.[7,8] Hence, substituted aromatic heterocyclic phosphate salts gradually attract people's attention both from academic and an industrial point of view. Research about the crystallization of iPP nucleated with sodium 2,2-methylene-bis (4,6-di-*tert*-butylphenyl) phosphate has been reported during the recent years.[1–5] Gui et al.[1] investigated the effects of sodium 2,2-methylene-bis (4,6-di-*tert*-butylphenyl) phosphate on crystallization behaviors and mechanical properties of iPP. Zhang et al.[2] studied the isothermal and nonisothermal crystallization kinetics of iPP nucleated with sodium salts and triglyceride of 2,2-methylene-bis (4,6-di-*tert*-butylphenyl) phosphate, and the results showed that the nucleation effects of sodium salts were better than those of triglyceride. Mai et al.[3,4] studied the crystallization behaviors of iPP nucleated by phosphate salts melting at different temperature for several minutes. But presently no literature reports the effects of an individual bivalent metal salt or trivalent salt as a nucleating agent on crystallization behaviors of iPP, and that whether they have the similar nucleation effects as sodium salts is unknown. So it is important to study the effects of bivalent and trivalent metal salts of substituted aromatic heterocyclic phosphate on crystallization behaviors of iPP, which will be beneficial to find the general rules of crystallization behavior of iPP nucleated with substituted aromatic heterocyclic phosphate salts and the nucleation mechanism of this type of nucleating agents in iPP so that to design novel nucleating agents with better nucleation effects. There are many literatures reporting the crystallization behaviors and kinetics of nucleated iPP.[1–5,9–14] Zhu et al.[9] studied the effects of alkali dehydroabietate on the crystallization of iPP by adopting Avrami method and

Correspondence to: Z. Xin (xzh@ecust.edu.cn).
Contract grant sponsor: SINOPEC

© 2006 Wiley Periodicals, Inc.

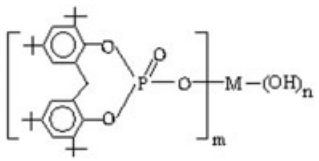

Name	NA11	NA03	NA19	NA20	NA12	NA30	NA13
M	Na	Li	K	Ca	Mg	Zn	Al
m	1	1	1	2	2	2	2
n	0	0	0	0	0	0	1

Scheme 1 Structure of nucleating agents in this study.

Hoffmann theory. Feng et al.[10] studied effects of dibenzylidene sorbitol on crystallization kinetics of iPP. But most of them are concerning the effects of one or two kinds of nucleating agents on crystallization of iPP.

The purpose of this article is to study the crystallization kinetics of iPP nucleated with different substituted aromatic heterocyclic phosphate salts systematically by a differential scanning calorimeter (DSC) under isothermal and nonisothermal conditions and to find the general nucleation rule of this type of nucleating agents in iPP. For isothermal crystallization, Avrami equation is generally used to describe the crystallization kinetics, while for nonisothermal crystallization, there are many methods such as Jeziorny method modifying Avrami equation,[15] Owaza method,[16] Mo method,[17] and Caze method.[18] In the former three methods the zero point selection of crystallization is involved while it has obvious effect on the calculated results, but in Caze method zero point selection of crystallization can be avoided, so in this article Caze method is chosen to describe the nonisothermal crystallization of iPP.

EXPERIMENTAL

Materials

An iPP pellets with a MFR of 2.5 g per 10 min, supplied by Yangzi Petrochemical (People's Republic of China), is used in this work. The nucleating agents prepared according to literature[19] are metal salts of substituted aromatic heterocyclic phosphate, and their structures are shown in Scheme 1.

Sample preparation and DSC analysis

The iPP pellets and a nucleating agent (0.2 wt %) were mixed in a high-speed mixer for 5 min. Then the mixture was extruded by an SJSH-30 twin-screw extruder through a strand die and pelletized. The pellets were molded into test specimens by a CJ-80E injection-molding machine.

The crystallization behaviors were investigated in isothermal and nonisothermal by using a Perkin–Elmer Diamond DSC (Perkin–Elmer Company, USA). All DSC operations were carried out under a nitrogen environment. Samples weights were between 2 and 3 mg and all samples were heated to 200°C and hold in the molten state for 5 min to erase their thermal history. In isothermal crystallization experiments, the sample melts were subsequently rapidly cooled to the crystallization temperature T_c and maintained until the crystallization of the matrix was completed. The exotherms were recorded at selected crystallization temperatures. Nonisothermal crystallization experiments were carried out by cooling samples from 200 to 50°C using different cooling rate. The exotherms were recorded with the cooling rates 5, 10, 20, 30, and 40°C/min, respectively.

Theory of crystallization

For isothermal crystallization Avrami model is a classical method and is widely used. The Avrami equation has been extended by Ozawa[16] to develop a simple method to study the nonisothermal experiment. The general form of Ozawa theory is written as follows:

$$X_v(T) = 1 - \exp(-K_T/\phi^m) \quad (1)$$

where K_T is the cooling crystallization function, Φ, the cooling rate, and m is the Ozawa exponent that depends on the dimension of the crystal growth. But there is a main hypothesis in Ozawa method that n is independent of temperature and only a limited number of X_v data are available for the foregoing analysis, as the onset of crystallization varies considerably with the cooling rate.

Caze et al.[18] put forward a new method to modify Ozawa equation. They have assumed an exponential increase of K_T with T upon cooling. On the basis, the temperatures at the peak and the two inflection points of the exotherm with skew Gaussian shape are linearly related to ln Φ to estimate the exponent n.

On the basis of the findings on the crystallization behavior of poly(ethylene terephthalate) and PP, Kim et al. proposed[20]

$$\ln K_T = a(T-b) \quad (2)$$

where a and b are empirical constants. If the extreme point of the pertinent $\partial X_v(T)/\partial T$ curve occurs at $T = T_q$ (crystallization peak temperature), i.e. $(\partial^2 X_v(T)/\partial T^2)_{T_q} = 0$, we have

$$K_T(T_q) = \phi^n \quad (3)$$

Combining eqs. (1)–(3) yields

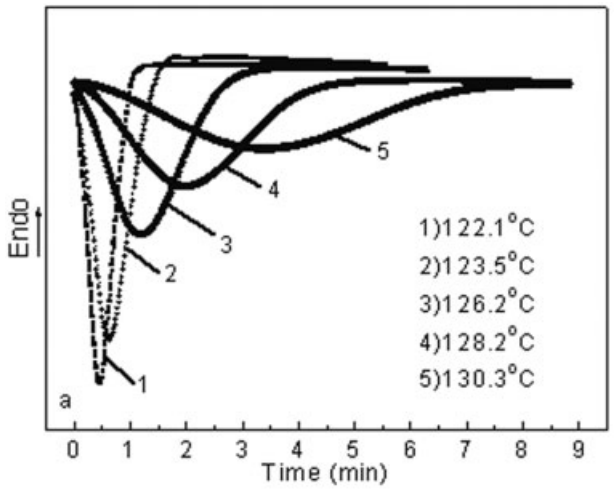

(a)

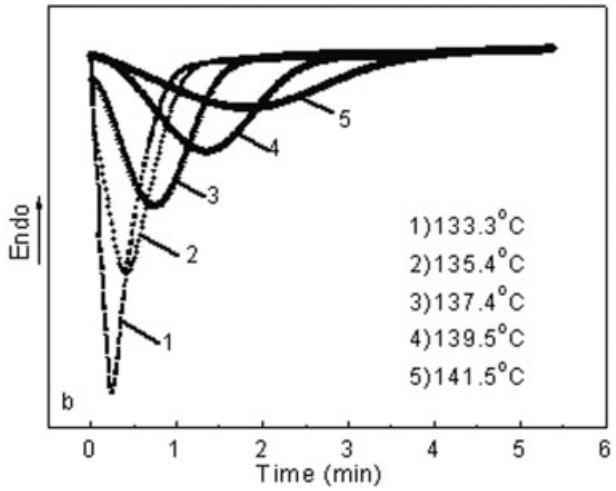

(b)

Figure 1 Heat flow curves of iPP (a) and iPP/NA11 (b) during isothermal crystallization.

$$\ln[-\ln(1 - X_v(T))] = a(T - T_q) \tag{4}$$

Hence, a linear plot of $\ln[-\ln(1-X_v(T))]$ against T would result in the constant a and the product $-aT_q$ from the gradient and intercept, respectively. At $T = T_q$ obtained from the foregoing algorithm, eqs. (3) and (4) lead to

$$T_q = n\ln\phi/a + b \tag{5}$$

As such, n can be obtained from the linear plot of T_q against $\ln \Phi/a$ in accordance with eq. (5).

RESULTS AND DISCUSSION

Isothermal crystallization of iPP nucleated with substituted aromatic heterocyclic phosphate salts

The studies of the isothermal crystallization behavior of virgin iPP and nucleated iPP are carried out by DSC at different temperatures. Figure 1 shows the heat flow evolution of iPP and iPP/NA11 for the isothermal crystallization obtained by rapidly cooling the molten polymer to the crystallization temperature, and those of iPP nucleated with other nucleating agents are similar. The effect of temperature on crystallization rate of iPP/NA11 is clearly observed in isothermal thermograms. With the increase in crystallization temperature, exothermal peak of DSC curves shifts right obviously, which indicates that crystallization time is increased and crystallization rate is decreased.

This effect is still more evident in the relative amount of crystallinity curves obtained by integration of the exothermal peaks, which are reported in Figure 2. The relative crystallinity, X_t, is expressed as

$$X_t = \frac{X_t(t)}{X_t(\infty)} = \frac{\int_0^t (dH(t)/dt)dt}{\int_0^\infty (dH(t)/dt)dt} \tag{6}$$

where $(dH(t)/dt)$ represents the heat flow, $X_t(t)$ and $X_t(\infty)$ denote the absolute crystallinity at time t and at the termination of the crystallization process, respectively.

From Figure 2 crystallization half-time $t_{1/2}$ can be obtained, and the results are listed in Table I. With the increasing crystallization temperature, crystallization half-time $t_{1/2}$ of iPP increases. In addition the incorporation of monovalent salts of substituted aromatic heterocyclic phosphate can decrease $t_{1/2}$ obviously while bivalent and trivalent salts have little effect on it.

Then the classical Avrami model can be used to analyze the development of the relative crystallinity in isothermal crystallization to the following equation[21,22]:

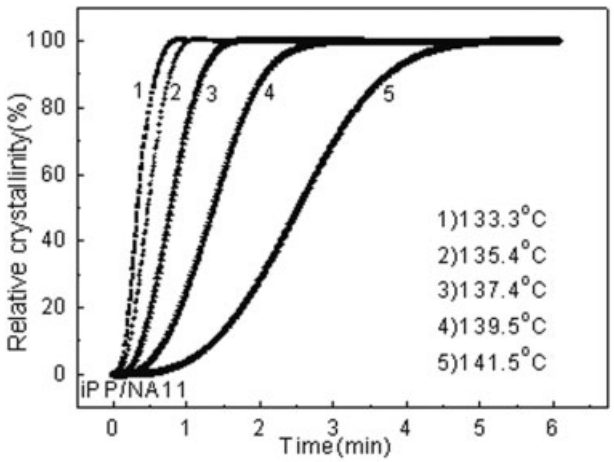

Figure 2 Relative crystallinity versus time for iPP/NA11 during isothermal crystallization.

TABLE I
Isothermal Crystallization Kinetic Parameters of iPP and Nucleated iPP

Sample	T_c (°C)	n	Z_t (min^{-n})	$t_{1/2}$[a] (s)	$t_{1/2}$[b] (s)	n (average)	K_g (10^5 K^2)	σ_e (J/m^2)
iPP	122.1	2.63	3.44	31	32	2.76 ± 0.08	9.01	0.150
	123.5	2.77	1.65	42	44			
	126.2	2.77	0.35	77	77			
	128.2	2.79	0.085	128	127			
	130.3	2.86	0.021	207	205			
iPP/NA11	133.3	2.72	10.70	20	22	2.84 ± 0.18	6.98	0.116
	135.4	2.61	4.66	29	29			
	137.4	2.86	1.41	47	47			
	139.5	2.93	0.28	82	82			
	141.5	3.06	0.04	151	152			
iPP/NA12	122.1	2.80	1.36	46	47	2.98 ± 0.13	9.02	0.150
	124.1	2.91	0.38	73	74			
	126.2	2.96	0.10	115	115			
	128.2	2.87	0.024	196	195			
	130.3	2.85	0.0046	350	349			
iPP/NA13	124.1	3.01	24.28	17	18	3.01 ± 0.13	8.97	0.149
	126.2	2.81	3.97	28	31			
	128.2	3.04	1.16	47	51			
	130.3	3.06	0.26	79	82			
	132.3	3.15	0.045	142	142			
iPP/NA03	133.3	2.76	12.57	21	22	2.83 ± 0.10	6.71	0.112
	135.4	2.71	4.97	28	29			
	137.4	2.83	1.56	45	45			
	139.5	2.88	0.30	80	80			
	141.5	2.95	0.046	149	150			
iPP/NA19	133.3	2.73	10.72	20	22	2.83 ± 0.09	6.72	0.112
	135.4	2.75	4.66	30	30			
	137.4	2.82	1.30	48	48			
	139.5	2.90	0.28	82	82			
	141.5	2.93	0.045	152	152			
iPP/NA20	124.1	2.98	15.83	20	21	3.00 ± 0.04	8.97	0.149
	126.2	2.95	4.43	32	32			
	128.2	3.01	1.13	50	51			
	130.3	2.99	0.25	84	84			
	132.3	3.05	0.046	146	146			
iPP/NA30	124.1	3.02	8.66	25	26	3.04 ± 0.02	8.87	0.148
	126.2	3.05	2.58	38	39			
	128.2	3.07	0.96	54	54			
	130.3	3.03	0.20	89	90			
	132.3	3.05	0.041	151	151			

[a] Determined from Figure 2.
[b] Calculated from Avrami parameters.

$$1 - X_t = \exp(-Z_t t^n) \quad (7)$$

where n is the Avrami exponent, Z_t is the rate constant, and X_t is the relative crystallinity calculated with equation (6) at a different crystallization time, t. From the plot of $\ln[-\ln(1-X_t)]$ versus $\ln t$, the parameters of eq. (7) can be obtained by the conventional Avrami plot method. The typical Avrami plots obtained at various temperatures are illustrated for virgin iPP, iPP/NA11, iPP/NA12, and iPP/NA13 in Figure 3. Other samples have the similar Avrami plots. There are good linearities of $\ln[-\ln(1-X_t)]$ versus $\ln t$ in a wide relative crystallinity range. It is clear that the Avrami equation is quite successful for analyzing the experimental data of the isothermal crystallization kinetics. The Avrami exponent n and the rate constant Z_t can be obtained from the values of the slope and intercept of these straight lines. The values of Z_t, n and $t_{1/2}$ are listed in Table I.

For virgin iPP, an average value of $n = 2.76 \pm 0.08$ is obtained over the crystallization temperature range studied, which is close to the value 2.6 in literature.[2] This value can be attributed to a heterogeneous nucleation followed by diffusion-controlled spherulite growth due to the existence of impurities and catalyst residues.[23] While for nucleated iPP, n values are all

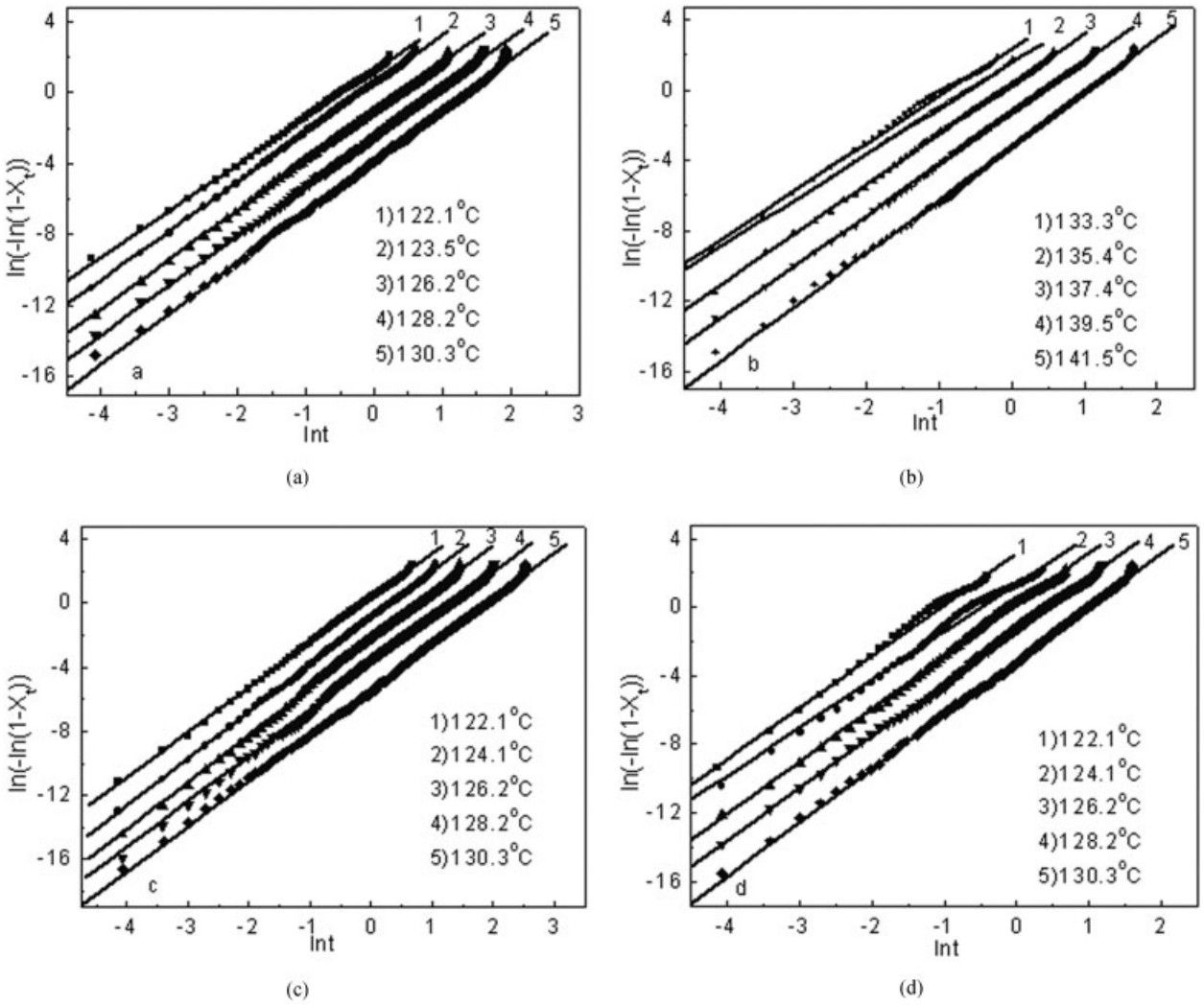

Figure 3 Plots of $\ln(-\ln(1-X_t))$ versus $\ln t$ for isothermal crystallization of (a) iPP, (b) iPP/NA11, (c) iPP/NA12, and (d) iPP/NA13.

close to 3, which indicate the addition of nucleating agents does not change the spherulite growth patterns of iPP. The average value of n for iPP/NA11is 2.84 ± 0.18, which is consistent with that in literature.[2]With the increase in crystallization temperature, crystallization rate constants of all samples are decreased, which indicates crystallization rate decreases with the increase in crystallization temperature. In addition, the addition of monovalent salts can shorten $t_{1/2}$ of iPP obviously, while bivalent and trivalent salts have little effect on crystallization rate of iPP. Yoshimoto et al.[5] utilized epitaxial crystallization to explain the nucleation effect of sodium 2,2-methylene-bis (4,6-di-*tert*-butylphenyl) phosphate (expressed as NA-11) on iPP. As the c cell dimension of iPP is very close to the b cell dimension of sodium 2,2-methylene-bis (4,6-di-*tert*-butylphenyl) phosphate, and further the a cell dimension of sodium 2,2-methylene-bis (4,6-di-*tert*-butylphenyl) phosphate is about four times the *a* value of iPP cell, the lattice matching is able to be performed between two crystal lattices, and then the following epitaxial crystallization will take place preferentially: $[010]_{\text{NA-11}}//[001]_{\text{iPP}}$ and $[001]_{\text{NA-11}}//[010]_{\text{iPP}}$. The free energy barrier of nucleation is reduced because of the existing of epitaxial crystallization, and then the rate of nucleation increases. The strong or weak nucleation ability of other metal salts of 2,2-methylene-bis (4,6-di-*tert*-butylphenyl) phosphate may result from whether there is crystal lattice matching between the nucleating agent and iPP, which we will study in further work. From the calculated and experimental $t_{1/2}$, we can conclude that the Avrami model is in agreement with the experimental data.

According to the Hoffman theory, the growth rate of crystals G can be expressed as follows[9,24]:

$$G = G_0 \exp\left[-\frac{U^*}{R(T_c - T_\infty)}\right] \exp\left[-\frac{K_g}{T_c \Delta T f}\right] \quad (8)$$

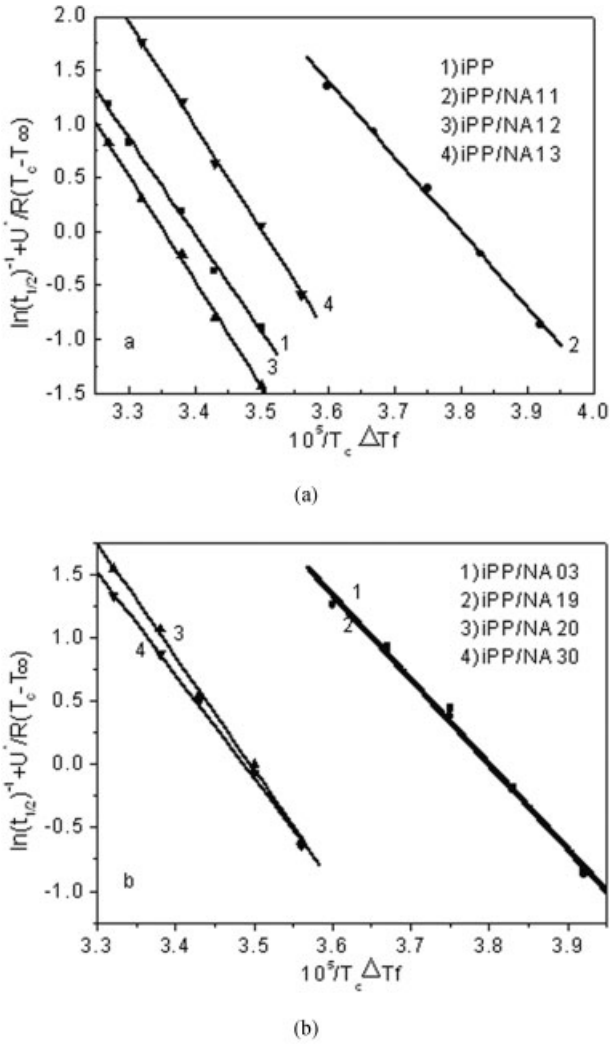

Figure 4 Plots of $\ln(t_{1/2})^{-1} + \frac{U^*}{R(T_c - T_\infty)}$ versus $1/(T_c\Delta Tf)$ for iPP and nucleated iPP: (a) iPP, iPP/NA11, iPP/NA12, iPP/NA13 and (b) iPP/NA03, iPP/NA19, iPP/NA20, iPP/NA30.

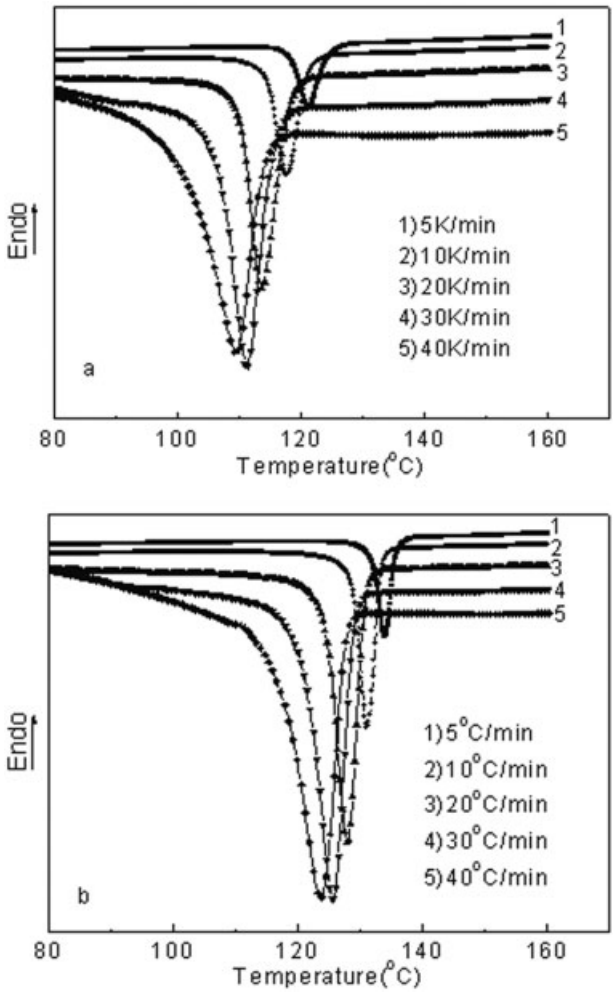

Figure 5 DSC cooling curves of (a) iPP and (b) iPP/NA11 during nonisothermal crystallization.

where G_0 is a preexponential factor containing quantities not strongly dependent on temperature, U^* is the activation energy of polymer segments transporting to the crystal front through the subcooled melt, and U^* is 6270 J/mol for iPP, R is the gas constant, T_∞ is the equilibrium melting temperature at which all motion associated with viscous flow ceases and is given by $T_g - 30$ K (T_g is 263 K for iPP), T_c is the crystallization temperature, ΔT is the degree of supercooling ($T_m^0 - T_c$), where T_m^0 is the equilibrium melting temperature (here ΔT_m^0 is 481 K for iPP), f is a correcting factor for variation in the heat of fusion with temperature and is approximated by $f = 2T_c/(T_m^0 + T_c)$, and K_g is the nucleation constant.

Assuming that the crystal growth mechanism of the polymer is as a three-dimensional spherulite, and the number of nuclei in isothermal crystallization is con-

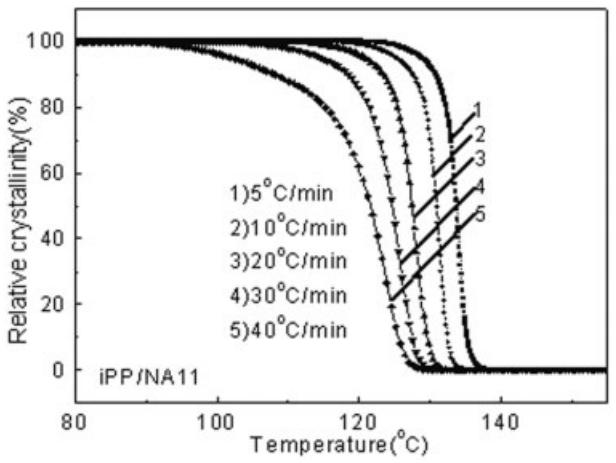

Figure 6 Relative crystallinity of iPP/NA11 at different cooling rate.

TABLE II
Nonisothermal Crystallization Kinetic Parameters for iPP and Nucleated iPP

Sample	Φ (°C/min)	T_p^a (°C)	a	T_q^b (°C)	$t_{1/2}$ (s)	n	ΔE (kJ/mol)
iPP	5	121.0	−0.89	121.0	80	3.71 ± 0.25	216
	10	117.6	−0.88	117.4	44		
	20	113.8	−0.76	113.3	25		
	30	111.0	−0.74	110.6	21		
	40	109.2	−0.73	108.7	15		
iPP/NA11	5	134.0	−1.35	133.4	46	3.17 ± 0.30	279
	10	131.2	−1.40	130.5	26		
	20	127.5	−1.21	126.8	14		
	30	125.6	−1.04	125.1	11		
	40	123.1	−0.85	122.5	8		
iPP/NA12	5	120.7	−1.02	120.4	85	3.18 ± 0.37	251
	10	118.0	−0.92	117.6	43		
	20	114.6	−0.83	114.7	24		
	30	112.9	−0.79	111.7	21		
	40	111.2	−0.77	110.3	14		
iPP/NA13	5	125.7	−1.38	125.4	54	3.21 ± 0.17	245
	10	122.8	−1.34	122.1	30		
	20	119.6	−0.99	119.2	20		
	30	116.9	−0.79	116.5	17		
	40	114.5	−0.79	113.5	12		
iPP/NA03	5	134.2	−1.38	133.7	48	3.20 ± 0.32	279
	10	131.3	−1.49	130.9	28		
	20	128.2	−1.33	127.6	16		
	30	125.8	−1.13	125.5	12		
	40	123.9	−1.04	123.5	10		
iPP/NA19	5	133.8	−1.44	133.6	48	3.02 ± 0.21	293
	10	131.8	−1.43	131.3	28		
	20	129.3	−1.36	129.0	17		
	30	126.6	−1.00	125.9	12		
	40	124.8	−0.88	124.1	10		
iPP/NA20	5	129.5	−1.22	129.3	76	3.13 ± 0.32	227
	10	126.1	−1.27	126.0	38		
	20	122.2	−1.00	122.2	26		
	30	119.4	−0.84	119.2	18		
	40	117.2	−0.71	116.3	15		
iPP/NA30	5	124.8	−1.46	124.6	68	3.17 ± 0.25	239
	10	121.9	−1.44	121.6	35		
	20	118.3	−1.24	118.0	24		
	30	115.6	−0.96	114.9	21		
	40	113.4	−0.79	113.1	13		

[a] Determined from Figure 5.
[b] Calculated from Caze method.

stant, the growth rate G is reciprocally proportional to the half-crystallization-time ($t_{1/2}$). Then we obtain

$$\ln(t_{1/2})^{-1} + \frac{U^*}{R(T_c - T_\infty)} = A - \frac{K_g}{T_c \Delta T f} \tag{9}$$

Thus, the plot of $\ln(t_{1/2})^{-1} + \frac{U^*}{R(T_c - T_\infty)}$ versus $1/(T_c \Delta T f)$ will give a straight line (Fig. 4), and K_g can be determined form the slope of the line. The results are listed in Table I.

The fold surface free energy σ_e can be obtained by the following equation:

$$K_g = \frac{4\sigma\sigma_e b_0 T_m^0}{k\Delta H} \tag{10}$$

where k is the Boltzman constant, b_0 is the thickness of the molecular layer and is determined by lattice parameters, $\triangle H$ is the theoretical heat of fusion, σ and σ_e are interfacial free energies per unit area parallel and perpendicular to the molecular chain direction, respectively. The value of σ can be obtained from the following expression:

$$\sigma = a b_0 \Delta H \tag{11}$$

where a is an empirical constant close to 0.1, b_0 is 6.56 $\times 10^{-10}$m and ΔH is 1.34 $\times 10^8$ J/m^3 for iPP, then the value of σ for iPP is 8.79 $\times 10^{-3}$ J/m^2, so the fold surface free energy σ_e can be directly obtained from K_g and the results are also listed in Table I. It can be seen that the addition of monovalent salts of substituted aromatic heterocyclic phosphate can decrease fold surface free energy σ_e obviously. The smaller the fold free energy of crystallization surface, the smaller the energy needed by macromolecule chain to form crystal structure on nuclei is, then the smaller the energy needed to reach the critical nuclei size is. So it can be regarded that the addition of monovalent salts can increase the nucleation and crystallization rate of iPP, while bivalent and trivalent salts have little effect on σ_e of iPP, that is to say, they have little effect on crystallization rate of iPP, which is consistent with the results obtained from Avrami method.

Nonisothermal crystallization of iPP nucleated with substituted aromatic heterocyclic phosphate salts

From a technological point of view, nonisothermal crystallization conditions approach more closely the industrial conditions of polymers processing, so that the study of crystallization of polymers under nonisothermal conditions is of great practical importance. The nonisothermal crystallization of iPP and nucleated iPP were carried out by DSC with cooling rates from 5 to 40°C/min. The thermograms of iPP and iPP/NA11 are reported in Figure 5 and those of iPP nucleated with other nucleating agents are similar. With increasing cooling rate, crystallization peak temperature of iPP (T_p) shifts to lower temperature. With the addition of monovalent metal salts of substituted aromatic heterocyclic phosphate, T_p of iPP is increased greatly. When cooling rate is 10°C/min, T_p of iPP/NA11 is increased from 121.0°C of virgin iPP to 133.4°C, while bivalent and trivalent metal salts of substituted aromatic heterocyclic phosphate have little effect on T_p of iPP.

By means of integrating the partial areas under the DSC endotherm, one would obtain the values of the crystalline weight fraction $X_w(T)$ (Fig. 6).

Crystallization half-time $t_{1/2}$ can be obtained from Figure 6 by using equation $t = (T_0 - T)/\phi$ (where t is crystallization time, T_0 is onset crystallization temperature, T is crystallization temperature and Φ is cooling rate). The results are listed in Table II. It can be seen that addition of monovalent metal salts of substituted aromatic heterocyclic phosphate can shorten $t_{1/2}$ of iPP increasingly. When cooling rate is 10°C/min, $t_{1/2}$ of iPP/NA11 can be decreased from 44 s of virgin iPP to 26 s, while bivalent and trivalent metal salts of substituted aromatic heterocyclic phosphate have little effect on $t_{1/2}$ of iPP.

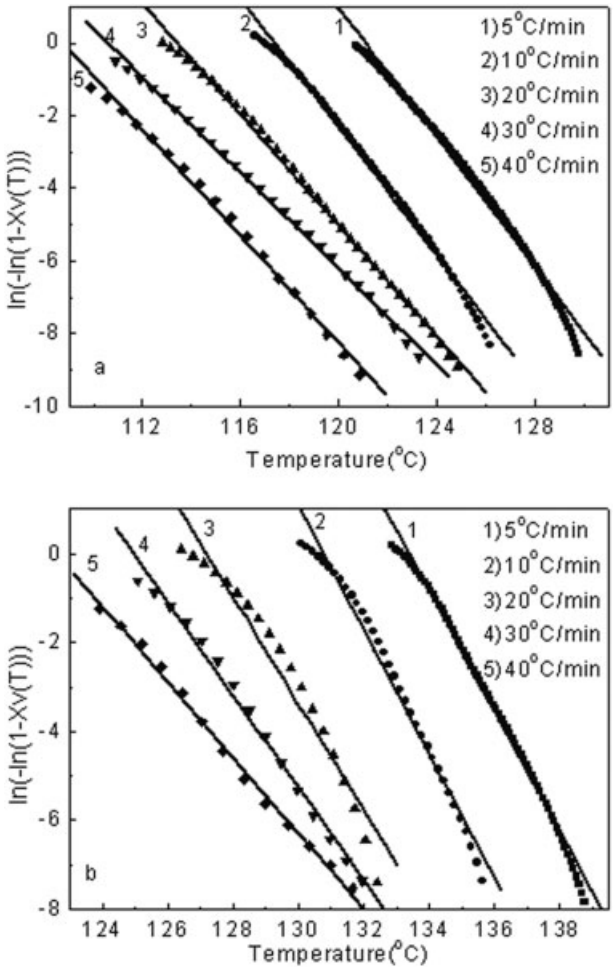

Figure 7 Plots of ln[−ln(1 − $X_v(T)$)] versus T for virgin (a) iPP and (b) iPP/NA11.

Now $X_w(T)$ can be converted into $X_v(T)$ by eq. (12)[20]:

$$X_v(T) = \frac{X_w(T)\frac{\rho_a}{\rho_c}}{1-(1-\rho_a/\rho_c)X_w(T)} \qquad (12)$$

where ρ_a and ρ_c are the bulk densities of the polymer in the amorphous and pure crystalline states, respectively. For iPP, the density of the amorphous phase is ρ_a = 0.852, and that of the crystallized phase is ρ_c = 0.935. So plots of ln[−ln(1 − $X_v(T)$] versus T can be obtained (Fig. 7) and there is good linear relationship between them. The values of a and $-aT_q$ can be determined from the slope and intercept of each straight line, and the results are also listed in Table II.

Straight lines can be obtained from plots of obtained T_q versus ln ϕ/a under different cooling rates (Fig. 8), and Avrami exponents of iPP and nucleated iPP can be determined from the slope of each straight line. The results are also listed in Table II.

As for iPP, the Avrami exponent is 3.71 closing to 4, which indicates that in virgin iPP the crystal growth

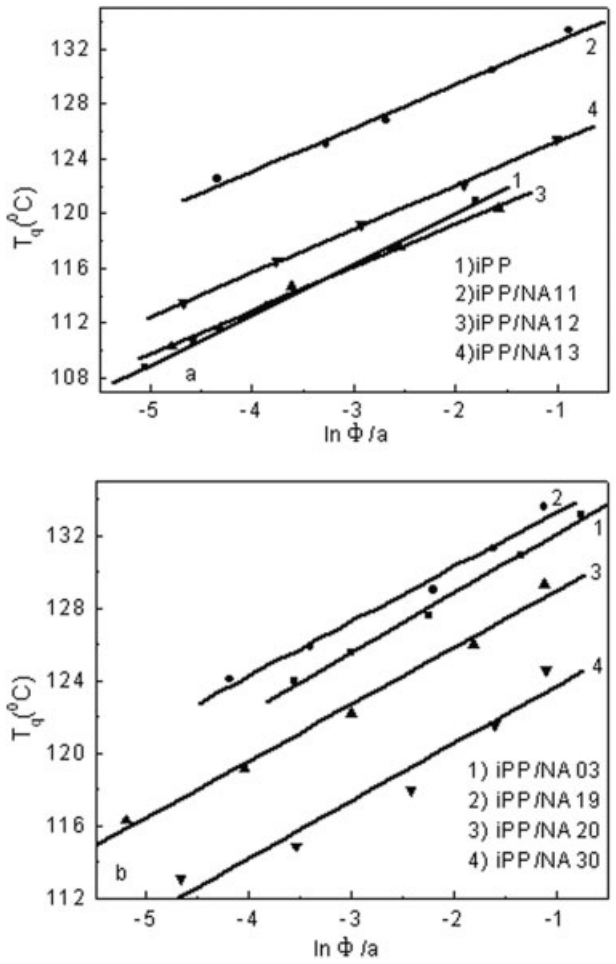

Figure 8 Plots of T_q versus ln ϕ/a for iPP and nucleated iPP: (a) iPP, iPP/NA11, iPP/NA12, iPP/NA13 and (b) iPP/NA03, iPP/NA19, iPP/NA20, iPP/NA30.

pattern is homogeneous nucleation followed by three-dimensional spherulite growth. While Avrami exponents of all nucleated iPP are close to 3, which indicates in nucleated iPP the crystal growth pattern is heterogeneous nucleation followed by three-dimension spherulite growth. Addition of all substituted aromatic heterocyclic phosphate salts can change the crystal growth pattern.

The Kissinger method can be used to determine the activation energy of nonisothermal crystallization of iPP and nucleated iPP[25]:

$$d[\ln(\phi)/T_p^2]/d(1/T_p) = -\Delta E/R \qquad (13)$$

where ϕ is cooling rate, T_p is the crystallization peak temperature, and R is the gas constant, ΔE is the activation energy of nonisothermal crystallization.

The plots of $\ln(\phi)/T_p^2$ against $1/T_p$ give a straight line (Fig. 9). According to the slope of each straight line, the crystallization activation energy of iPP and nucleated iPP can be calculated. The results are listed in Table II.

It can be seen that addition of different metal salts of substituted aromatic heterocyclic phosphate can increase the crystallization activation energy of iPP. It indicates that addition of nucleating agents plays a role of heterogeneous nuclei, on the other hand, the strong interaction between molecule chain of nucleating agents and that of iPP will hinder the crystallization of iPP.[26] But in crystallization process consisting of nucleation and growth, nucleation rate plays a control role on crystallization process. Although addition of nucleating agents increases the crystallization activation energy of iPP, total crystallization rate is increased because nucleation rate is accelerated greatly due to the existence of large amounts of heterogeneous nuclei.

CONCLUSIONS

The crystallization kinetics of iPP nucleated with substituted aromatic heterocyclic phosphate salts have

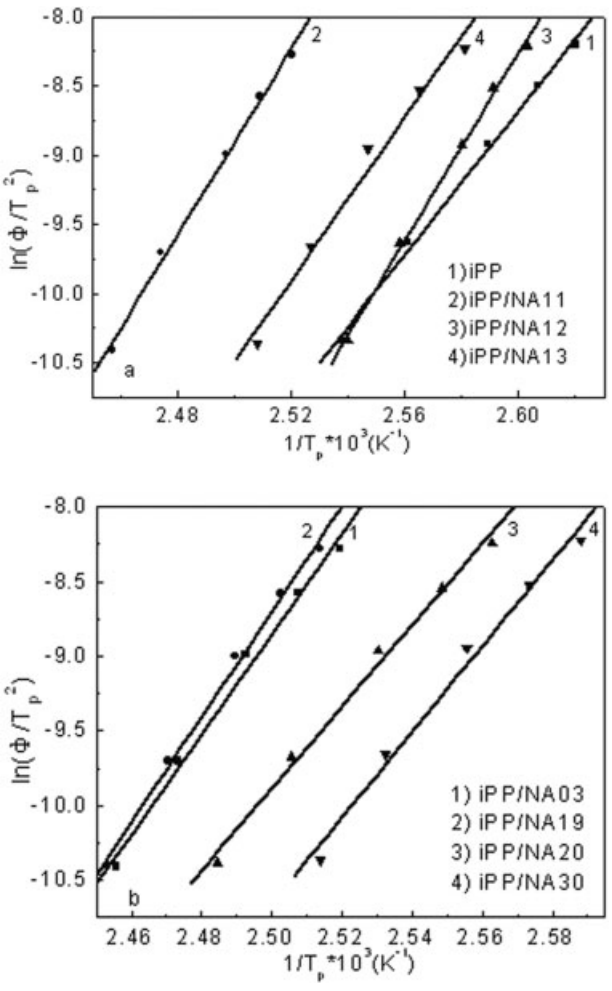

Figure 9 Plots of $\ln(\phi/T_p^2)$ versus $1/T_p$ for iPP and nucleated iPP: (a) iPP, iPP/NA11, iPP/NA12, iPP/NA13 and (b) iPP/NA03, iPP/NA19, iPP/NA20, iPP/NA30.

been investigated under isothermal and nonisothermal conditions by Avrami method and Caze method, respectively. Under both conditions, the addition of monovalent salts of substituted aromatic heterocyclic phosphate can increase the crystallization rate and decrease crystallization half-time of iPP remarkably while bivalent and trivalent salts have little effect. Under isothermal conditions the Avrami equation is successfully employed to deal with the crystallization kinetics, meanwhile the addition of monovalent phosphate salts can decrease the interfacial free energy per unit area perpendicular to PP chains σ_e value of iPP. The Caze method is successfully employed to deal with the nonisothermal crystallization kinetics. Under nonisothermal conditions the addition of nucleating agents changes the spherulite growth pattern of iPP. For virgin iPP growth pattern is homogeneous nucleation followed by three-dimensional spherulite growth, while for iPP nucleated with substituted aromatic heterocyclic phosphate salts growth pattern is heterogeneous nucleation followed by three-dimension spherulite growth. In addition the introduction of nucleating agents can increase crystallization activation energy of iPP.

References

1. Gui, Q. D.; Xin, Z.; Zhu, W. P.; Dai, G. C. J Appl Polym Sci 2003, 88, 297.
2. Zhang, G. P.; Yu, J. Y.; Xin, Z.; Gui, Q. D.; Wang, S. Y. J Macromol Sci Phys 2003, B42, 663.
3. Mai, K. C.; Wang, K. F.; Han, Z. W.; Zeng, H. M. J Appl Polym Sci 2002, 83, 1643.
4. Mai, K. C.; Wang, K. F.; Han, Z. W.; Zeng, H. M. J Appl Polym Sci 2001, 81, 78.
5. Yoshimoto, S.; Ueda, T.; Yamanaka, K.; Kawaguchi, A.; Tobita, E.; Haruna, T. Polymer 2001, 42, 9627.
6. Akio, S.; Hirokazu, N. Eur. Pat. 280297 (1988).
7. Eisuke, S.; Koichi, Y. Jpn. Pat. 2003306586 (2003).
8. Tobita, E.; Urushibara, T.; Shimizu, T.; Kawamoto, N. Jpn. Pat. 2003335968 (2003).
9. Zhu, G.; Li, C. C.; Li, Z. Y. Eur Polym J 2001, 37, 1007.
10. Feng, Y.; Jin, X.; Hay, J. N. J Appl Polym Sci 1998, 69, 2089.
11. Kim, Y. C.; Kim, C. Y. Polym Eng Sci 1991, 31, 1009.
12. Marco, C.; Ellis, G.; Gomez, M. A.; Arribas, J. M. J Therm Anal Calorim 2002, 68, 61.
13. Mohmeyer, N.; Muller, B.; Behrendt, N.; Hillenbrand, J.; Klaiber, M. Polymer 2004, 45, 6655.
14. Beck, H. N.; Ledbetter, H. D. J Appl Polym Sci 1965, 9, 2131.
15. Jeziorny, A. Polymer 1978, 19, 1142.
16. Ozawa, T. Polymer 1971, 12, 150.
17. Liu, T. X.; Mo, Z. S.; Wang S. E.; Zhang H. F. Polym Eng Sci 1997, 37, 568.
18. Caze, C.; Devaux, E.; Crespy, A.; Cavrot, J. P. Polymer 1997, 38, 497.
19. Xin, Z.; CN. Pat. 1358728, (2002).
20. Kim, P. C.; Gan, S. N.; Chee, K. K. Polymer 1999, 40, 253.
21. Avrami, M. J Chem Phys 1939, 7, 1103.
22. Avrami, M. J Chem Phys 1940, 8, 212.
23. Lopez, M. M. A.; Biagiotti, J.; Torre, L.; Kenny, J. M. Polym Eng Sci 2000, 40, 2194.
24. Hoffman, J. D. Polymer 1983, 24, 3.
25. Zhu, X.; Yan, D. Colloid Polym Sci 2001, 279, 546.
26. Chen, W. Y.; Lin, Z. Y.; Yang, J.; Qian, H.; Huang, L. D. China Synth Resin Plast 2005, 22, 20.